VIP Conductive TiO_2

DOI: 10.1002/anie.200902207

Semimetallic TiO_2 Nanotubes**

*Robert Hahn, Felix Schmidt-Stein, Jarno Salonen, Stefan Thiemann, YanYan Song, Julia Kunze, Vesa-Pekka Lehto, and Patrik Schmuki**

The highly defined morphology of self-organized anodic TiO_2 nanotube layers found in recent years has applications in fields such as biotechnology,[1,2] photo-catalysis,[3,4] or dye-sensitized solar cells.[5] While the semiconducting nature of TiO_2 is crucial for many of these applications, the limited conductivity prevents an even broader and efficient use in applications that require a fast electron transport, such as functional electrodes or as electrocatalyst supports. Herein we demonstrate how to overcome this limitation by using a robust carbo-thermal reduction treatment converting the TiO_2 into an oxy carbide compound that shows stable semimetallic conductivity. These TiO_xC_y nanotubes can be used, for example, as an inert electrode with substantial overpotential for O_2 evolution, or as a highly efficient support for electrocatalytic reactions, such as in methanol-based fuel cells.

To produce TiO_2 nanotube layers we use self-organizing electrochemical anodization,[6–9] a process leading to oxide nanotubes on a range of refractory metals (e.g. titanium,[10] zirconium, hafnium[11,12]). TiO_2 in its anatase or rutile form is a wide band-gap semiconductor material ($E_g \approx 3.0$–3.2 eV) and as such particularly suitable for applications based on UV- or X-ray-induced interactions.[13] To achieve enhanced control over the electronic and optical properties of these semiconducting nanotubes, various doping approaches with suitable elements, for example, C[14,15] and N,[16–18] or various transition metals[19] were reported. However, for high-throughput electrodes, or electrocatalyst supports, the conventional doping approaches do not provide sufficient electrical conductivity. Herein we use a high-temperature treatment in acetylene that converts the semiconducting anatase phase into carbon rich (Magnéli-type) phases that show semimetallic conductivity. The process can be carried out without loss of the ordered nanotubular morphology as illustrated in Figure 1. In this case self-organized TiO_2 nanotubes were grown with a diameter of 80 nm to a layer

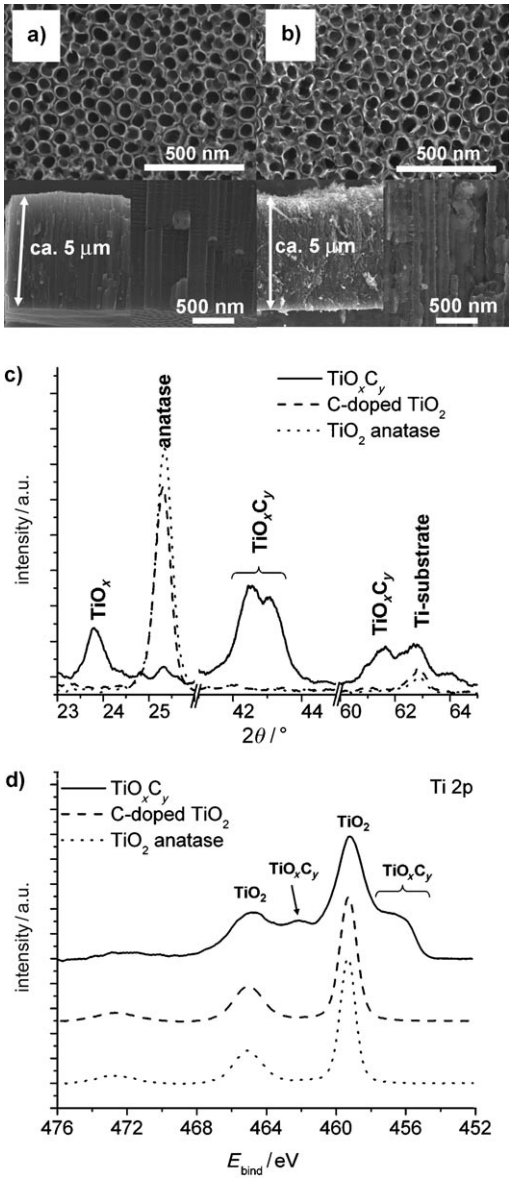

Figure 1. SEM images of the nanotubes after a) anodization formation and b) after a thermal acetylene treatment at 850 °C for 10 min. The lower insets are the corresponding cross-sectional views. c) X-ray diffraction results for the acethylene-treated tubes and those of anatase TiO_2 nanotubes and highly C-doped TiO_2 nanotubes. d) XPS spectra showing the Ti 2p peak of thermal-carbonized nanotubes and of anatase TiO_2 nanotubes and highly C-doped TiO_2 nanotubes.

[*] Dipl.-Ing. R. Hahn, Dipl.-Ing. F. Schmidt-Stein, S. Thiemann, Dr. Y. Y. Song, Dr. J. Kunze, Prof. Dr. P. Schmuki
University of Erlangen-Nuremberg
Department of Materials Science and Engineering
Martenstrasse 7, 91058 Erlangen (Germany)
Fax: (+49) 9131-852-7582
E-mail: schmuki@ww.uni-erlangen.de
Dr. J. Salonen, Dr. V.-P. Lehto
Laboratory of Industrial Physics, Department of Physics
University of Turku, 20014 Turku (Finland)

[**] We thank Prof. Allan Bard for drawing our attention to Magnéli phases. Furthermore the authors would like to acknowledge R. Kosmala for TEM, R. Lynch for SEM, U. Marten-Jahns for assistance in XRD and the Engineering of Advanced Materials (EAM) (catalysis section) Cluster of Excellence in Erlangen for financial support.

Supporting information for this article is available on the WWW under http://dx.doi.org/10.1002/anie.200902207.

thickness of 5 μm using an anodization process, and annealed in air at 450 °C to form anatase crystal structure (details are given in the Supporting Information). These layers were then treated in acetylene at 850 °C to trigger the desired carbonization reaction. After the treatment (Figure 1b) the nanotube layers only show some minor morphology changes, that is, the tubular shape is well maintained during the carbonization process. Figure 1c shows the most significant peaks of the X-ray diffraction (XRD) patterns (the full spectrum is given in the Supporting Information) before and after acetylene treatment.

The observed diffraction peaks can be attributed to the formation of titanium oxy carbide (TiC_xO_y), which is a solid solution of TiO in TiC and various TiO_2 suboxides. This result is also consistent with some TEM observations shown in the Supporting Information. These titanium oxy carbide species have been observed as intermediates, in addition to various suboxides (Ti_4O_7, Ti_3O_5, and Ti_2O_3), during the reduction of TiO_2 to form TiC.[20,21]

In addition, after acetylene treatment, a significant hardening of the layers through the carbon uptake was observed. To illustrate the differences to a conventional TiO_2 carbon-doping process[22] we included for comparison XRD data of TiO_2 nanotubes that were only C-doped by an acetylene treatment at 500 °C.[15] When using this classic, simple doping, clearly the characteristic TiO_xC_y peaks at $2\theta \approx 42.5°$, 61.5° are completely absent. The significant difference between C-doping and TiO_xC_y conversion also becomes evident from the X-ray photoelectron spectra (XPS) data (Figure 1d). Clear changes can be seen in the Ti 2p peak. The peak shifts show the formation of oxy carbides and the partial reduction of Ti^{4+} to Ti^{3+}.[23] An evaluation of the total composition of Ti:O:C revealed changes from an atomic ratio of 1:2.2:0.25 for the anatase nanotubes produced in an organic electrolyte to 1:1.6:3.8 after the high-temperature acetylene reaction. Further differences between doping and conversion are also evident in the XPS C 1s and O 1s peaks (see Supporting Information). An evaluation of the oxy carbide amount based on the O 1s region yields a ratio of oxy carbide to oxide of approximately 2.5:1. Solid-state electrical measurements are shown in Figure 2a for the anatase tubes, the C-doped TiO_2 tubes and TiO_xC_y nanotube layers. Results for different metal contacts (using sputter evaporated Al or Pt dots) are shown in the Supporting Information.

Clearly, the carbon-modified tubes show an ohmic I–V behavior for which the resistance is several orders of magnitude lower than for the carbon-doped or pure-anatase TiO_2 nanotubes. A rough estimate yields approximate conductivity values of $3 \times 10^5\ S\,m^{-1}$ for TiO_xC_y, $9 \times 10^4\ S\,m^{-1}$ for C-doped TiO_2, and $10^3\ S\,m^{-1}$ for anatase TiO_2 nanotubes.

A clear difference between semiconducting and semimetallic behavior is also evident using liquid electrolyte contacts. Capacity measurements at 1 kHz in 0.1 M Na_2SO_4 are plotted in Figure 2b according to a Mott–Schottky approach.[24] Also in these measurements, the anatase and the C-doped nanotubes reveal a voltage dependence of the capacity which is typical for the space charge layer controlled capacity of a n-type semiconductor in contact with an electrolyte. The evaluation of flatband potentials yields values of −270 mV (anatase) and of −490 mV (C-doped material). In contrast, the capacity of the TiO_xC_y electrode system has metallic behavior with only a weak dependence of the capacitance on the applied voltage, that is, a capacitance solely determined by the Helmholtz layer at the solid–liquid interface and therefore no reasonable flatband potential can be extracted. Moreover, from the photocurrent data in Figure 2c it is evident that for the anatase and C-doped materials a typical response of a semiconductor is observed whereas for the semimetal a completely different optical behavior (with a strong IR response) is obtained.

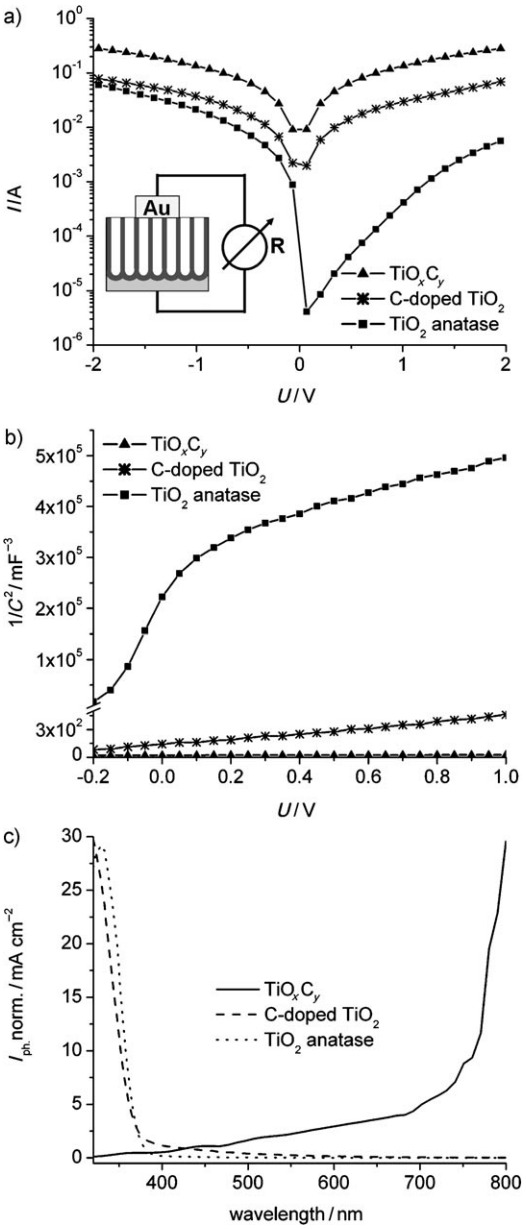

Figure 2. a) I–V characteristics of 2-point solid-state measurements of carbonized tubes and of anatase TiO_2 nanotube layers and C-doped layers. Inset: a simplified sketch of the 2-point measurement arrangement. b) Potential-dependent capacity measurements of the different nanotube layers in 0.1 M Na_2SO_4 solution at 1 kHz and plotted in a Mott–Schottky graph. c) Electrochemical photocurrent measurement of the nanotube layers in 0.1 M Na_2SO_4 at 500 mV versus Ag/AgCl.

Some examples of the strongly enhanced performance of the carbonized nanotubes as a conductive electrode material for electrochemistry are shown in Figure 3.

The cyclic voltammetry results in Figure 3a show the behavior of carbon modified tubes with a flat platinum foil and conventional anatase TiO_2 nanotubes in a defined redox electrolyte. The TiO_xC_y nanotube electrode clearly shows similarly defined oxidation and reduction peaks as a pure platinum electrode with electron-transfer kinetics that are orders of magnitude higher than for semiconducting anatase TiO_2. In fact, the anatase TiO_2 nanotube electrode shows only negligible reactions at these anodic overvoltages owing to the blocking character that is an inherent characteristic for an n-type semiconductor under anodic bias.[25]

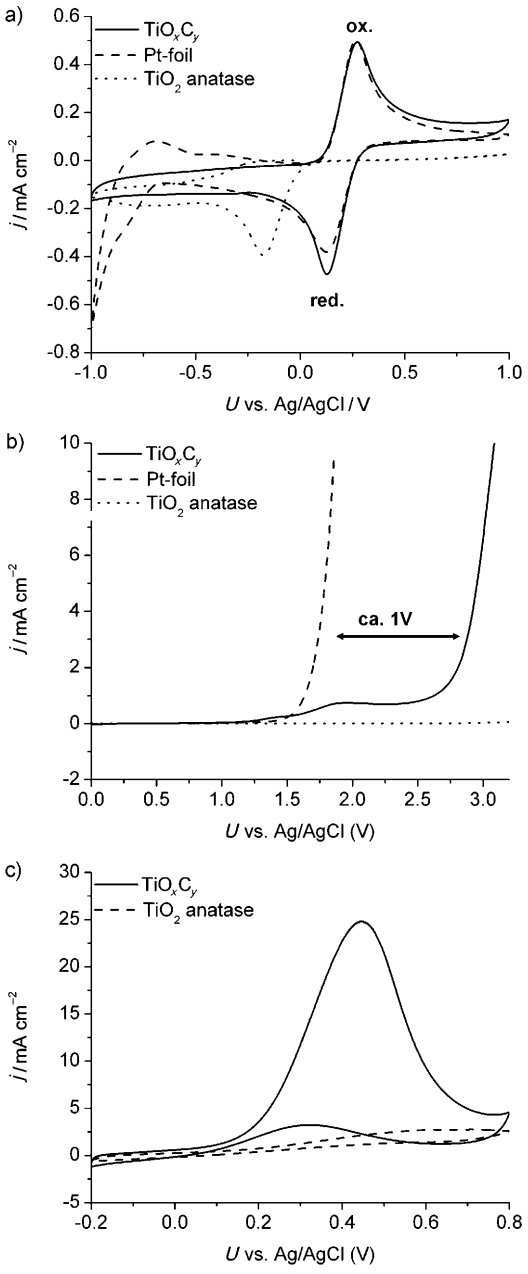

Figure 3. Electrochemical characterization: a) cyclic voltammetry results of carbonized nanotubes, anatase TiO_2 nanotubes, and a flat Pt foil in 5 mM $[Fe(CN)_6]^{-2/-3}$ solution. b) Polarization curves of the samples in 1 M H_2SO_4 illustrating the high overpotential for O_2 evolution. c) Cyclic voltammogram for the electrocatalytic oxidation of methanol from a 1 M CH_3OH + 1 M H_2SO_4 solution by using TiO_xC_y and anatase TiO_2 loaded under same conditions with Pt/Ru nanoparticles (500 μg cm^{-2}).

The oxy carbide electrodes also showed a high cycling stability as shown in the Supporting Information in Figure S4.

The electrodes have a large overpotential to oxygen evolution (Figure 3b). The small current increase between 1.5 V and 2.5 V may be ascribed to minimal oxide formation on oxy carbide phases.[26]

To give another example for an electrochemical reaction that requires an enhanced "potential window" we selected a reaction relevant to methanol-based fuel cells, that is the Pt/Ru catalyzed oxidation of methanol (usually performed on carbon substrates).[27,28] While previous work demonstrated that conventional anatase TiO_2 nanotubes can serve as a very beneficial support for methanol oxidation,[29] we show in Figure 3c that the use of conductive TiO_xC_y enhances (under the same catalyst loading conditions) the catalytic activity for methanol oxidation by 700%. Furthermore, for the semimetallic support the oxidation peak is much more defined. This simply reflects the strongly enhanced electron transfer across the support.

Overall, herein we demonstrate the successful conversion of TiO_2 in a nanotube array into a highly conductive and stable TiO_xC_y phase by a simple, one step, high-temperature treatment in acetylene. We obtain a highly functional and robust nanotubular electrode material with a very well defined and controllable morphology. The combination of semimetallic conductivity with a high overpotential for O_2 evolution makes the material, among other applications, suitable as a catalytic support for methanol fuel cells or other applications that require high electron conductivity.

Received: April 24, 2009
Revised: June 6, 2009
Published online: September 1, 2009

Keywords: carbon doping · conductivity · electrodes · nanotubes · TiO_2

[1] J. Park, S. Bauer, K. von der Mark, P. Schmuki, *Nano Lett.* **2007**, *7*, 1686–1691.
[2] Y. Y. Song, F. Schmidt-Stein, S. Bauer, P. Schmuki, *J. Am. Chem. Soc.* **2009**, *131*, 4230–4232.
[3] A. Fujishima, T. N. Rao, D. A. Tryk, *J. Photochem. Photobiol. C* **2000**, *1*, 1–21.
[4] M. R. Hoffmann, S. T. Martin, W. Choi, D. W. Bahnemann, *Photocatal. Chem. Rev.* **1995**, *95*, 69–96.
[5] T. Stergiopoulos, A. Ghicov, V. Likodimos, D. S. Tsoukleris, J. Kunze, P. Schmuki, P. Falaras, *Nanotechnology* **2008**, *19*, 235602.
[6] H. Masuda, K. Fukuda, *Science* **1995**, *268*, 1466–1468.
[7] J. M. Macák, H. Tsuchiya, P. Schmuki, *Angew. Chem.* **2005**, *117*, 2136–2139; *Angew. Chem. Int. Ed.* **2005**, *44*, 2100–2102.
[8] J. M. Macak, H. Tsuchiya, L. Taveira, S. Aldabergerova, P. Schmuki, *Angew. Chem.* **2005**, *117*, 7629–7632; *Angew. Chem. Int. Ed.* **2005**, *44*, 7463–7465.

[9] P. S. Albu, A. Ghicov, J. M. Macak, P. Schmuki, *Phys. Status Solidi RRL* **2007**, *1*, R65 – R67.
[10] V. Zwilling, E. Darque-Ceretti, A. Boutry-Forveille, D. David, M. Z. Perrin, *Alloy Surf. Interface Anal.* **1999**, *27*, 629 – 637.
[11] J. M. Macák, H. Tsuchiya, A. Ghicov, K. Yasuda, R. Hahn, S. Bauer, P. Schmuki, *Curr. Opin. Solid State Mater. Sci.* **2007**, *11*, 3 – 18.
[12] A. Ghicov, P. Schmuki, *Chem. Commun.* **2009**, 2791 – 2808.
[13] F. Schmidt-Stein, R. Hahn, J.-F. Gnichwitz, Y. Y. Song, N. K. Shrestha, A.Hirsch, P. Schmuki, *Electrochem. Commun.* **2009**, accepted.
[14] J. H. Park, S. Kim, A. J. Bard, *Nano Lett.* **2006**, *6*, 24 – 28.
[15] R. Hahn, A. Ghicov, J. Salonen, V.-P. Lehto, P. Schmuki, *Nanotechnology* **2007**, *18*, 105604.
[16] A. Ghicov, J. M. Macak, H. Tsuchiya, J. Kunze, V. Haeublein, L. Frey, P. Schmuki, *Nano Lett.* **2006**, *6*, 1080 – 1082.
[17] J. M. Macak, A. Ghicov, R. Hahn, H. Tsuchiya, P. Schmuki, *J. Mater. Res.* **2006**, *21*, 2824 – 2828.
[18] A. Ghicov, B. Schmidt, J. Kunze, P. Schmuki, *Chem. Phys. Lett.* **2007**, *433*, 323 – 326.
[19] A. Ghicov, M. Yamamoto, P. Schmuki, *Angew. Chem. Int. Ed.* **2008**, *47*, 7934 – 7937.
[20] R. Koc, J. S. Folmer, *J. Mater. Sci.* **1997**, *32*, 3101 – 3111.
[21] Y. Gotoh, K. Fujimura, M. Koike, Y. Ohkoshi, M. Nagura, K. Akamatsu, S. Deki, *Mater. Res. Bull.* **2001**, *36*, 2263 – 2275.
[22] S. Sakthivel, H. Kisch, *Angew. Chem.* **2003**, *115*, 5057 – 5060; *Angew. Chem. Int. Ed.* **2003**, *42*, 4908 – 4911.
[23] J. J. Blackstock, C. L. Donley, W. F. Stickle, D. A. A. Ohlberg, J. J. Yang, D. R. Stewart, R. S. Wiliams, *J. Am. Chem. Soc.* **2008**, *130*, 4041 – 4047.
[24] A. J. Bard, M. Stratmann, M. S. Licht, *Encyclopedia of Electrochemistry*, Vol. 6, Wiley-VCH, Weinheim, **2002**.
[25] H. Gerischer, *Electrochim. Acta* **1990**, *35*, 1677 – 1699.
[26] M. Zweynert, H. Döring, J. Garche, K. Enghardt, K. Wiesener, *Chem. Ing. Tech.* **1998**, *70*, 827 – 841.
[27] Z. D. Wei, S. H. Chan, *J. Electroanal. Chem.* **2004**, *569*, 23.
[28] A. Bauer, E. L. Gyenge, C. W. Oloman, *Electrochim. Acta* **2006**, *51*, 5356 – 5364.
[29] J. M. Macak, P. J. Barczuk, H. Tsuchiya, M. Z. Nowakowska, A. Ghicov, M. Chojak, S. Bauer, S. Virtanen, P. J. Kulesza, P. Schmuki, *Electrochem. Commun.* **2005**, *7*, 1417 – 1422.

